

Data S3: Analysis of Mass and Flow Cytometry, Repertoire and Proteomics, Related to STAR Methods

Related to **STAR Methods**: [Mass cytometry data analysis](#); [Flow cytometry data analysis](#); [Repertoire analysis](#); [Pre-processing and analysis of surface protein \(ADT\) data](#); [Luminex data analysis](#); and [Tims-TOF mass spectrometry analysis](#).

Table of Contents

Mass cytometry	3
1: Gating strategy for clean-up.....	3
2: Gating strategy for doublets exclusion.....	4
3: Flow-chart describing the analytical pipeline for the analysis of the mass cytometry data.	5
4: Whole blood (non-depleted) assayed by single cell mass cytometry (CyTOF).	6
5: Principal components analysis (PCA) of whole blood (non-depleted) assayed by single cell mass cytometry (CyTOF).	7
6: Whole blood (depleted) assayed by single cell mass cytometry.....	9
7: Myeloid cell populations from whole blood (depleted) assayed by single cell mass cytometry.....	10
8: Single cell mass cytometry (CyTOF) compositional analysis showing UMAP, clustering and differential abundance of major B cell populations.	12
9: Phenotype of the T/NK cell populations assayed by single cell mass cytometry.	13
Multicolor flow cytometry analysis	14
10: Phenotype and frequency of subsets of memory CD4 T cell subsets defined based on the expression of CCR4, CCR6 and CXCR3.....	14
Repertoire analysis	15
11: UMAP embedding B cell repertoire analysis (A) UMAP embedding with cluster identities from CITE-seq (B) UMAP embedding of all B cells from single cell VDJ dataset.	15
12: Illustration of the method used to identify CDR3 Kmers associated with COVID-19 compared to cells from healthy volunteers and patients with sepsis.....	16
13: Cluster proportions	17
14: Mean plasmablast diversity indices by comparator group; clonal expansion index, CEI, clonal diversification index, CDI.	18
15: Correlation analysis of IGHV genes detected by single cell VDJ data and RNA VDJ data, within the (top) IGHD/M unmutated, (middle) IGHD/M mutated and (bottom) class-switched VDJ sequences.	19
16: Volcano plots of log ₂ fold change of IGHV gene usage of IGHD/M unmutated sequences (derived from single cell VDJ data), IGHD/M mutated sequences (derived from RNA VDJ data), class-switched sequences (derived from RNA VDJ data).....	20
17: Proportion of constant region genes across B cell clusters per study group.....	21
18: Clonal overlap across comparator groups with total number of convergent clones per group shown with clonal network depicting distribution of convergent clusters (inset) and sequence logos of COVID-19 exclusive clusters (with IGHV/J usage and number of members).	22
19: Cumulative bar chart of the frequencies of known SARS-CoV-2 binding BCRs per patient group.	23
Proteomics	24

20: Clustering of surface protein (ADT) data24

21: Plasma protein abundance for specific proteins assayed by Luminex assay.25

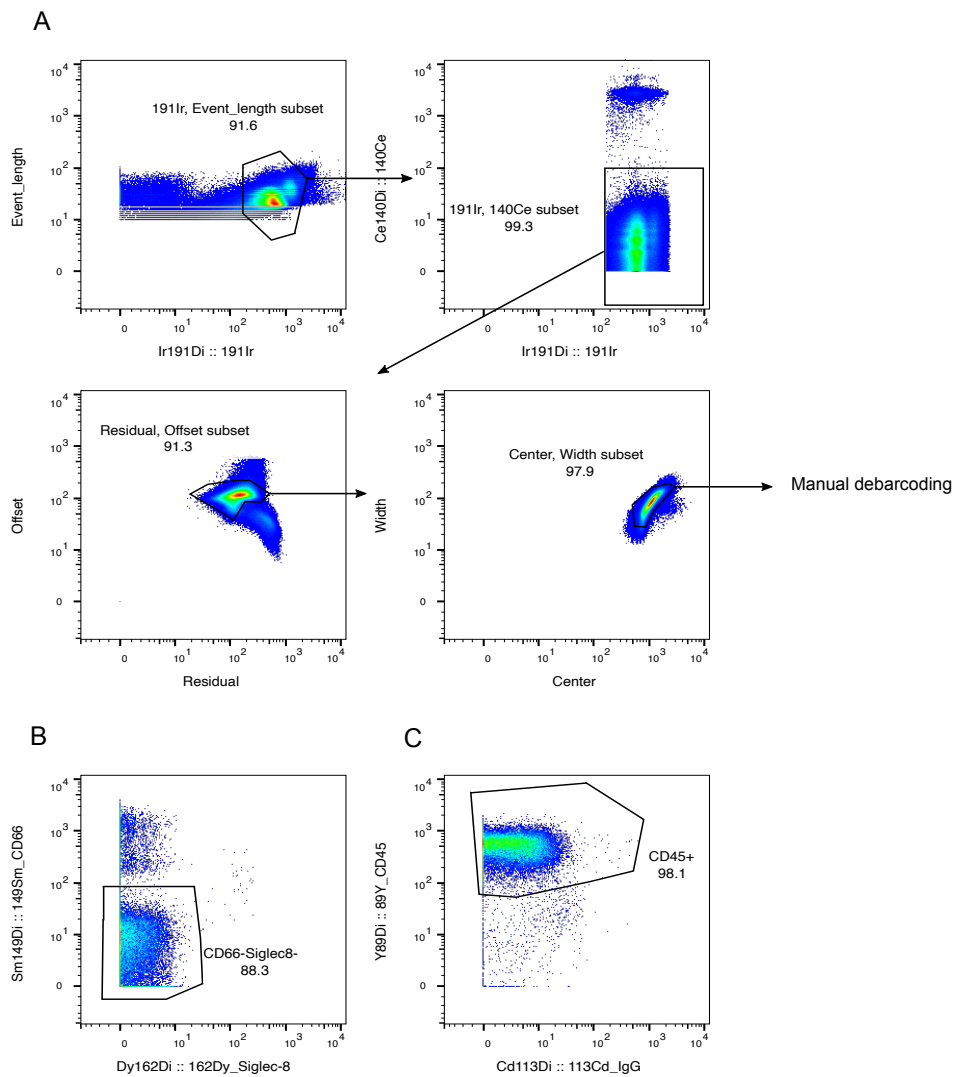
22: Heat map showing abundance of plasma and serum proteins by disease groups assayed using Luminex26

23: UMAP of plasma proteins assayed by Luminex assay, colored by comparator group.27

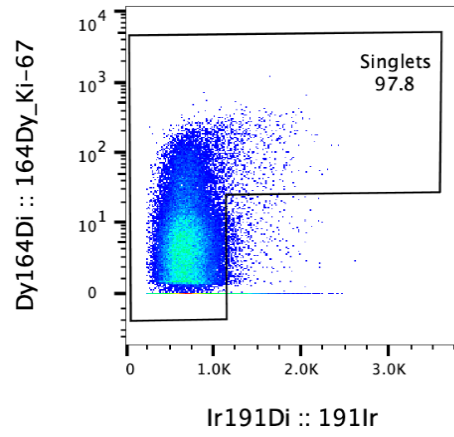
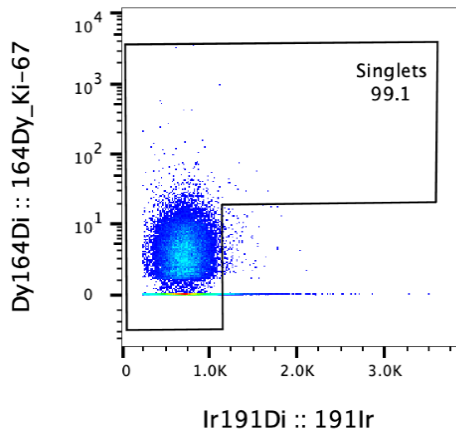
24: Unsupervised hierarchical clustering and supervised correlation analysis of plasma proteins assayed by HT-LC-MS/MS mass spectrometry.28

25: Plasma protein abundance for specific proteins assayed by HT-LC-MS/MS mass spectrometry.29

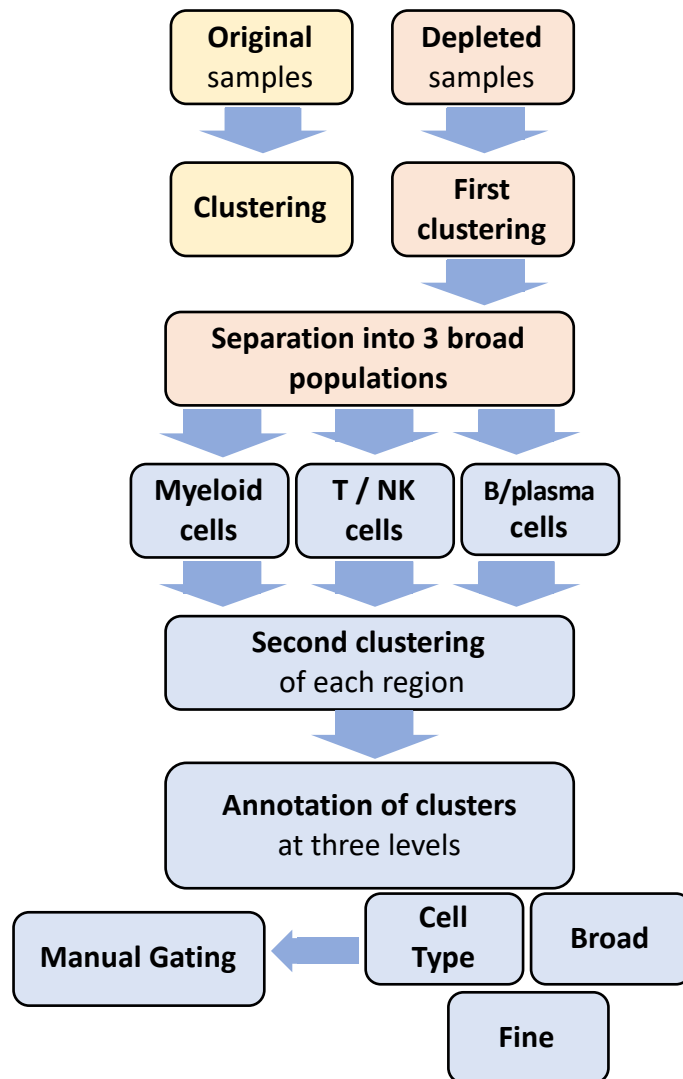
Mass cytometry



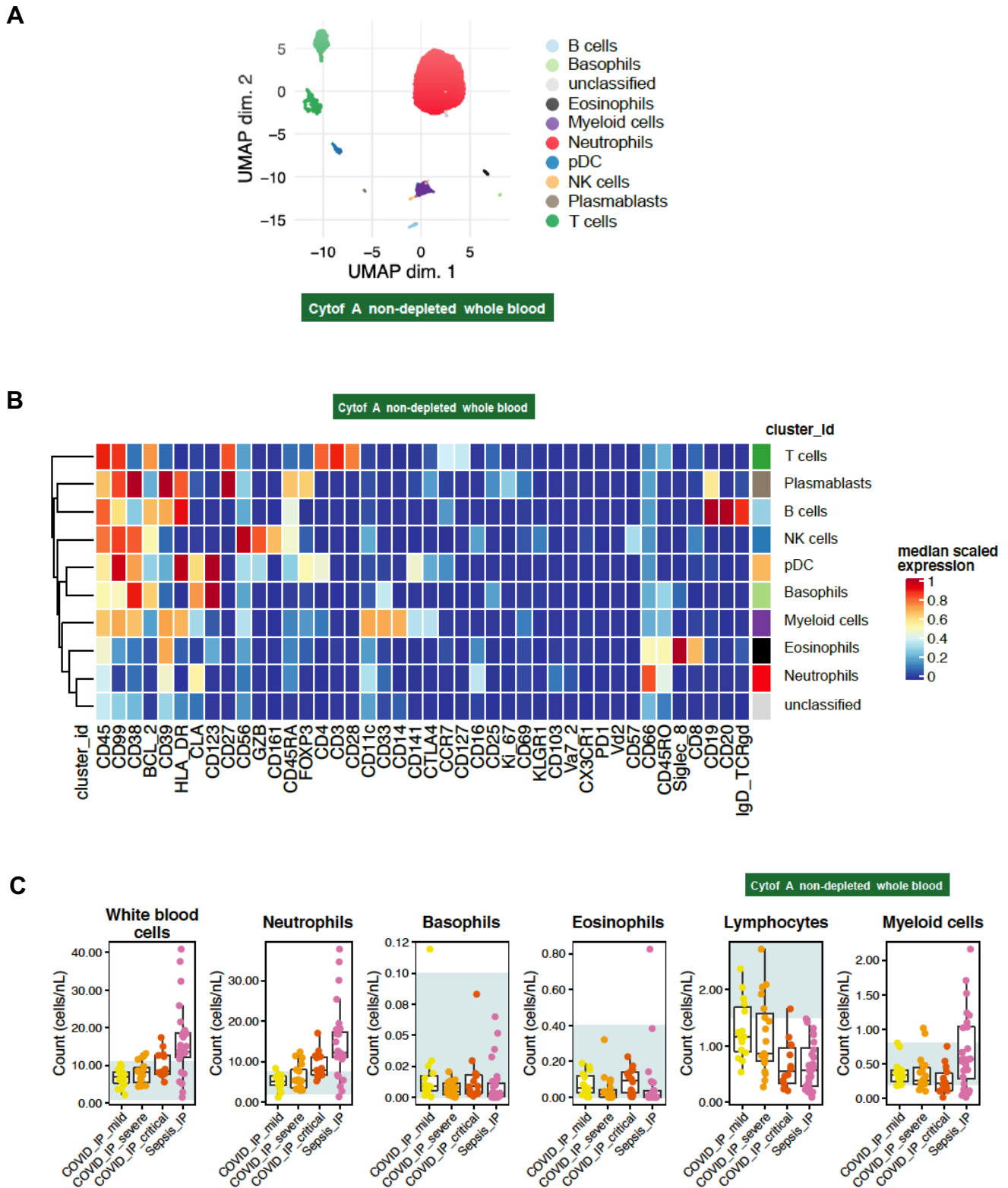
1: Gating strategy for clean-up. A Gating strategy for removal of beads, DNA negative events and for Gaussian parameters clean-up prior to Manual Debarcoding. **B** Clean up step to remove residual CD66+ granulocytes and Siglec-8 Eosinophils, in granulocytes depleted samples. This step was followed by gating of CD45+ cells. **C.** Gating of CD45+ cell for subsequent analysis. This step was performed for both depleted and non-depleted (original) samples. Related to STAR Methods: Mass cytometry data analysis: CyTOF data pre-processing.



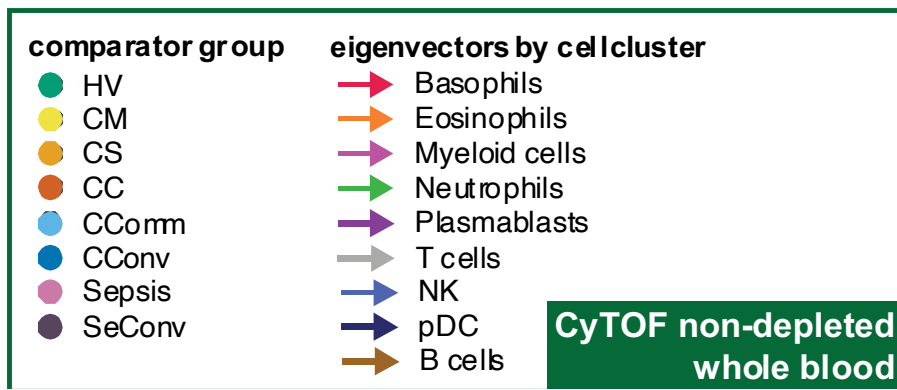
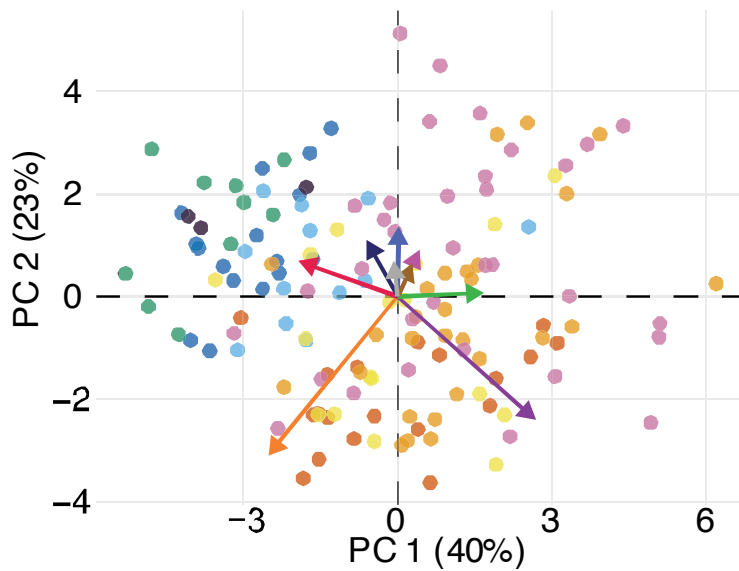
2: Gating strategy for doublets exclusion. Representative scatter plots showing DNA content on x-axis (191Ir - Iridium) versus the proliferation marker Ki67 on y-axis. The sample on the right shows a population of proliferating Ki67⁺ cells absent on the sample on the left. To not exclude proliferating cells from the analysis, the gating was made excluding only Iridium^{high}Ki67⁻ cells. Related to STAR Methods: Mass cytometry data analysis: CyTOF data pre-processing.



3: Flow-chart describing the analytical pipeline for the analysis of the mass cytometry data.
 Related to STAR Methods: Mass cytometry data analysis: clustering.

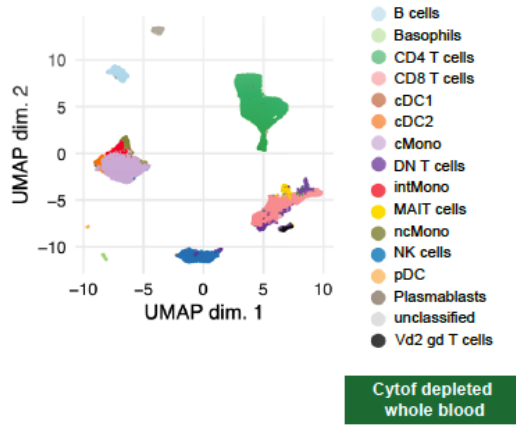


4: Whole blood (non-depleted) assayed by single cell mass cytometry (CyTOF). Non-granulocyte depleted samples. A self-organizing map algorithm (FlowSOM) resolved 25 clusters by consensus clustering for 3,893,390 cells after down sampling to a maximum of 40,000 cells. Clusters merged to identify broad immune cell populations (A) UMAP (B) clustering of major cell populations (y axis) by discriminating marker (x-axis) (C) cell counts by patient group. Related to STAR Methods: Mass cytometry data analysis: differential abundance analysis.

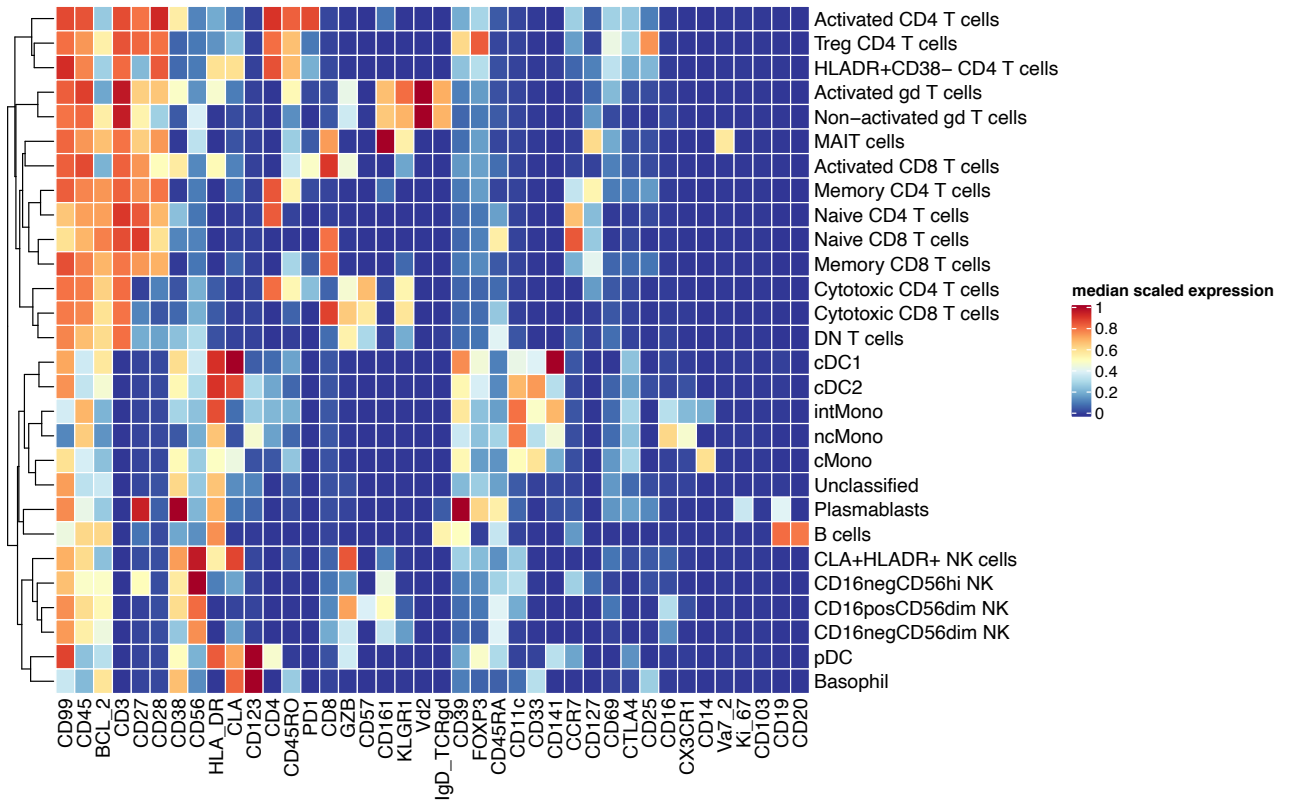


5: Principal components analysis (PCA) of whole blood (non-depleted) assayed by single cell mass cytometry (CyTOF). Major cell populations in whole blood for clinical comparator groups showing for non-granulocyte depleted samples PCA with arrows indicating drivers of variation by cell population. Related to STAR Methods: Mass cytometry data analysis: differential abundance analysis.

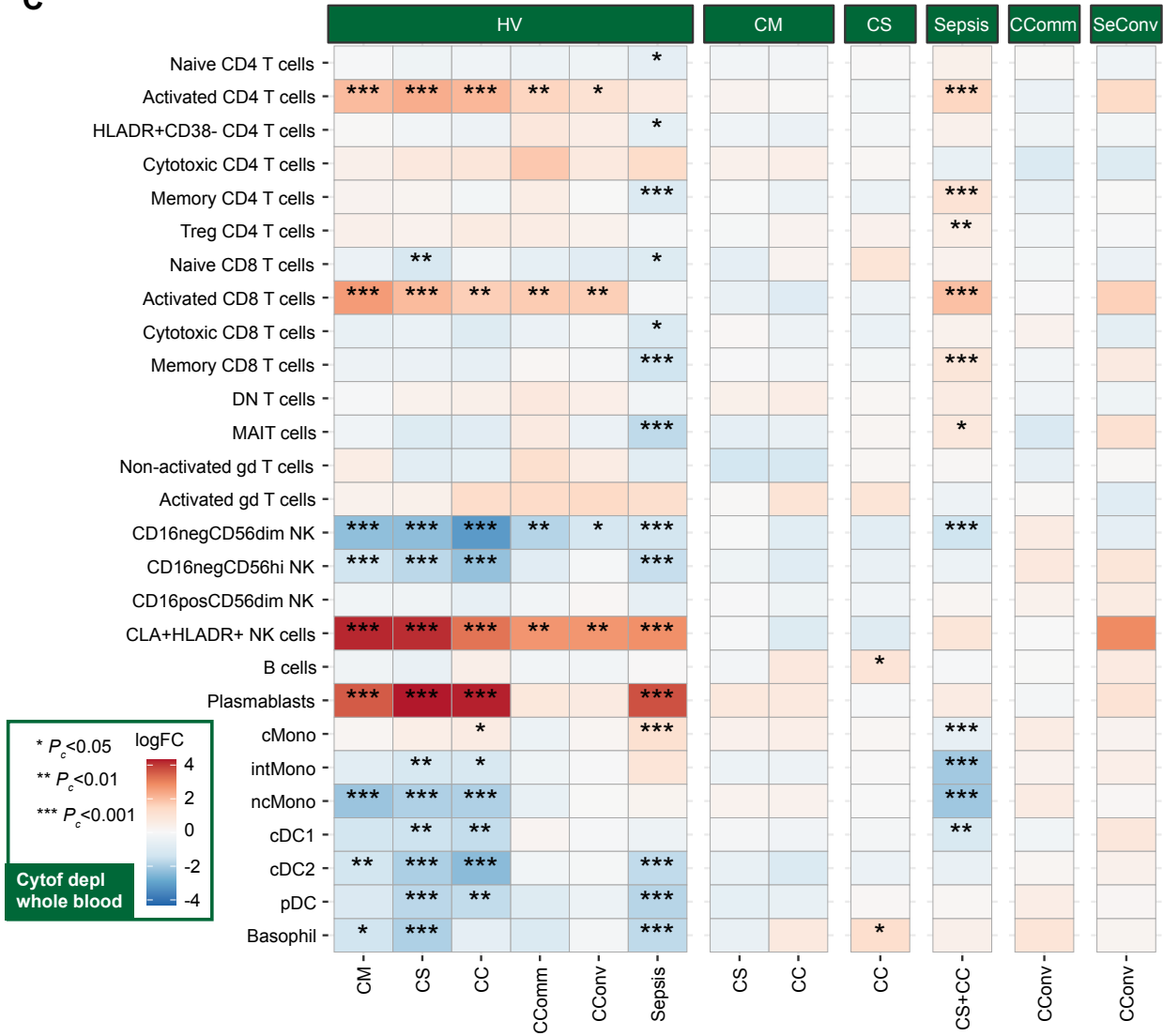
A



B

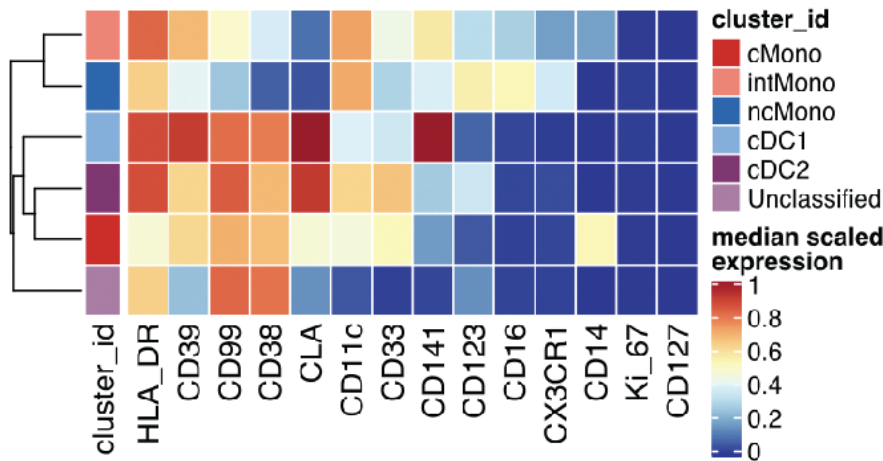


C

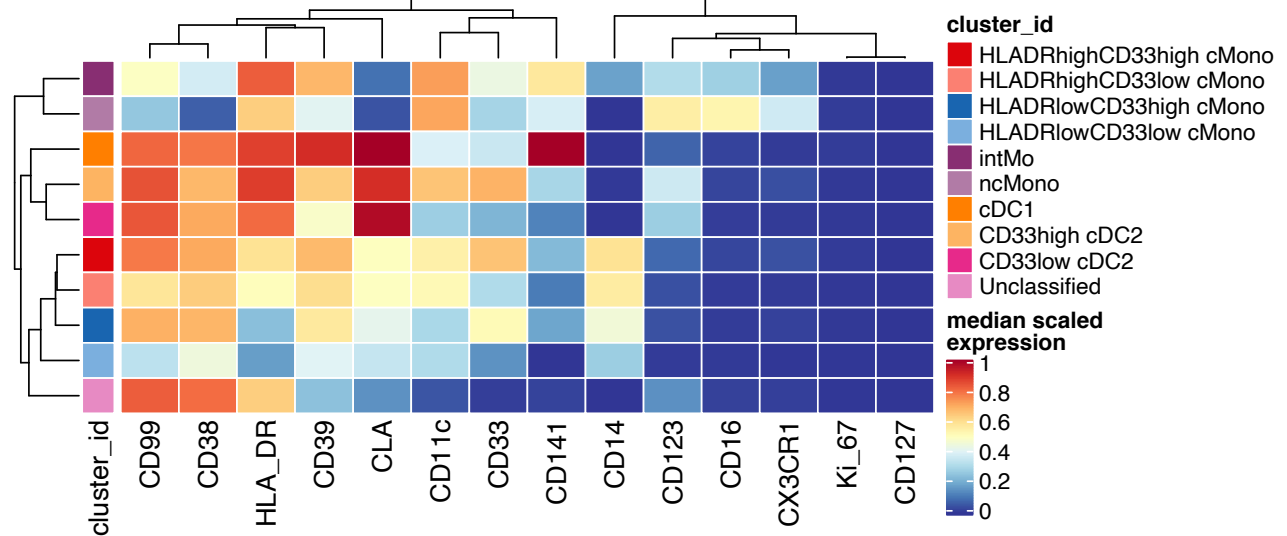


6: Whole blood (depleted) assayed by single cell mass cytometry. Heatmap showing the phenotype of broad cell populations for single cell mass cytometry (CyTOF) of granulocyte (CD66+) depleted whole blood with 7,118,158 cells assayed. (A) UMAP (B) clustering of major cell populations (y axis) by discriminating marker (x-axis) (C) differential abundance analysis. Related to STAR Methods: Mass cytometry data analysis: differential abundance analysis.

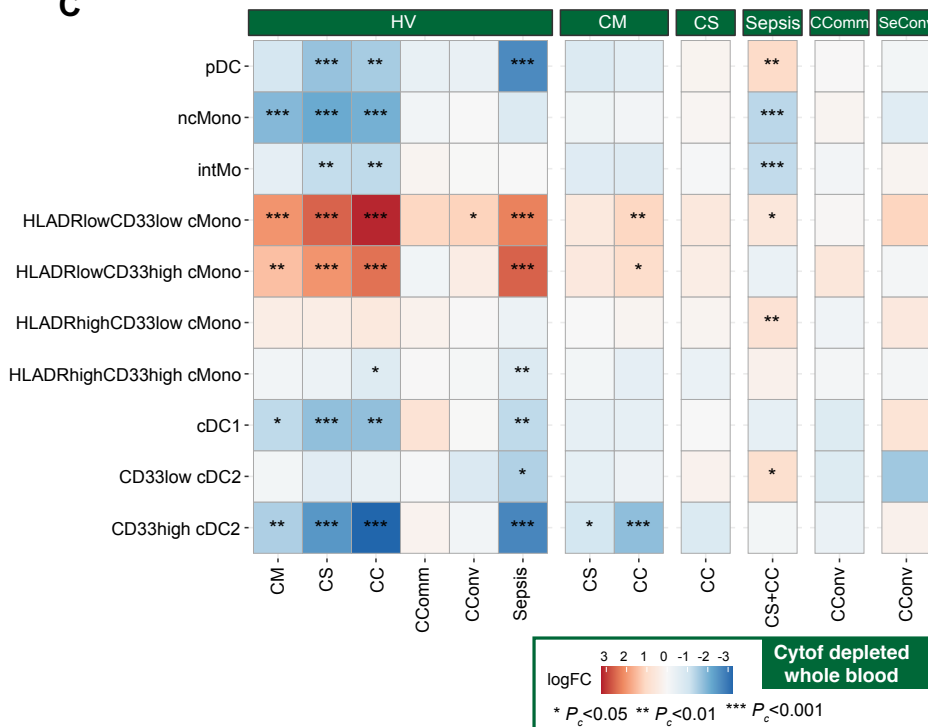
A



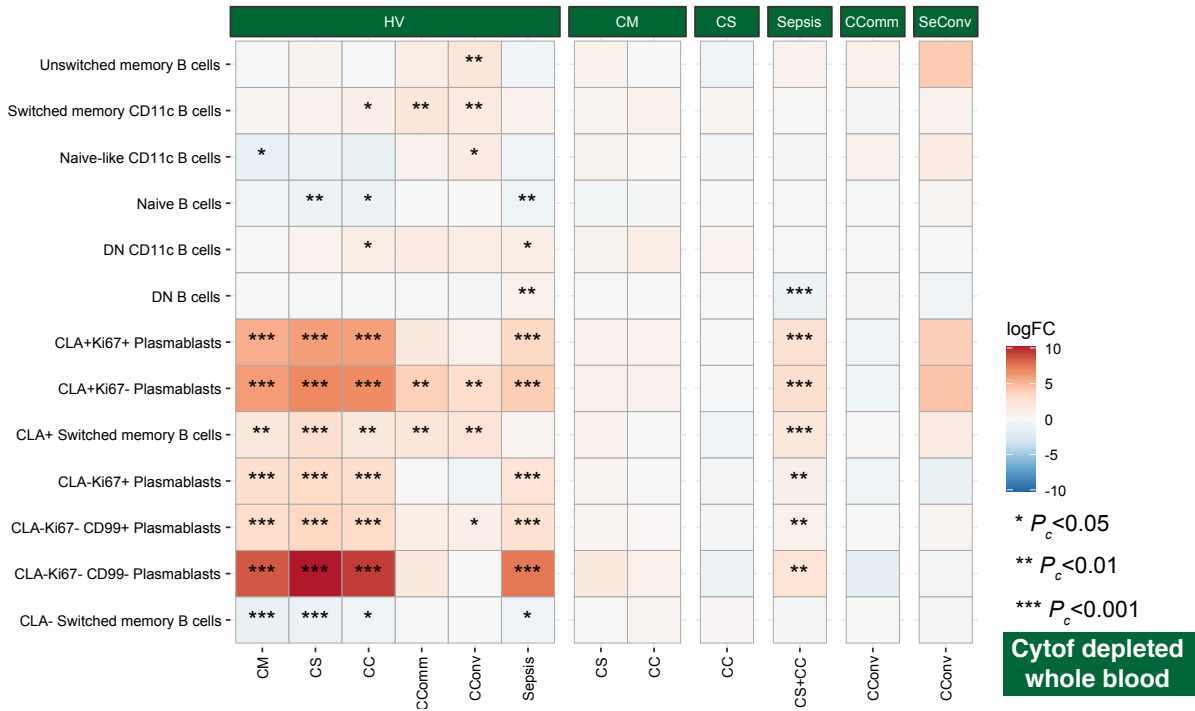
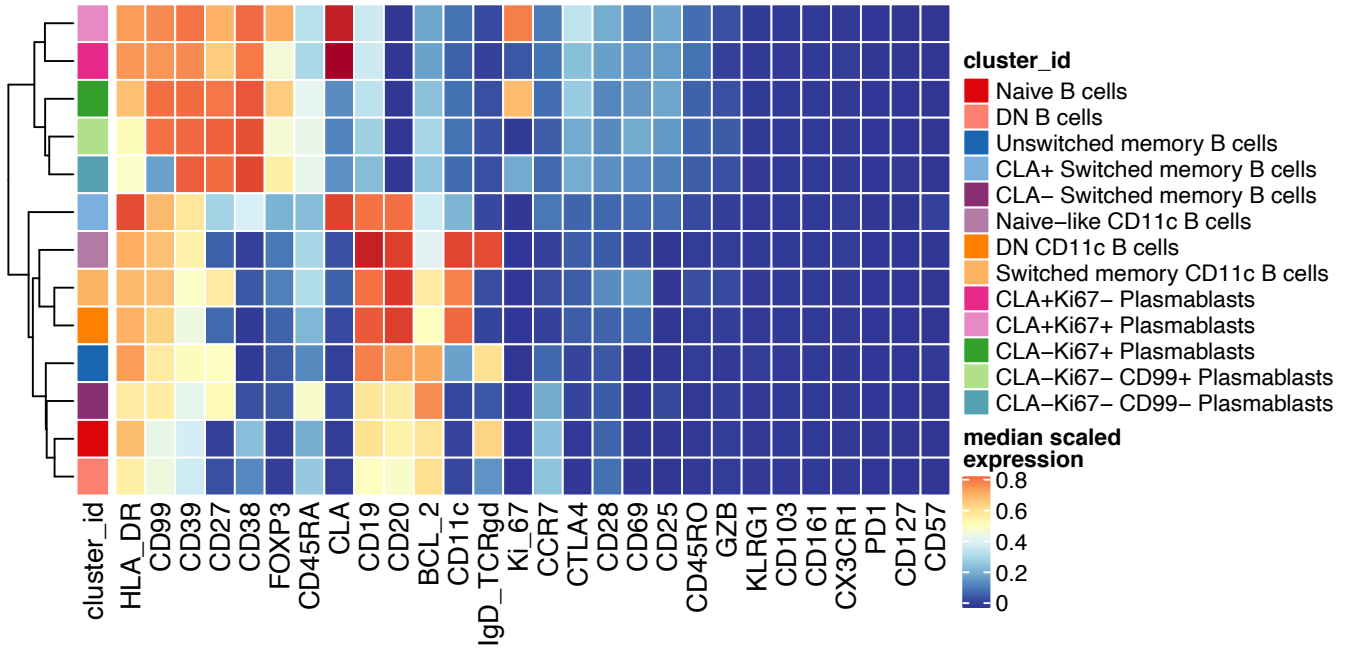
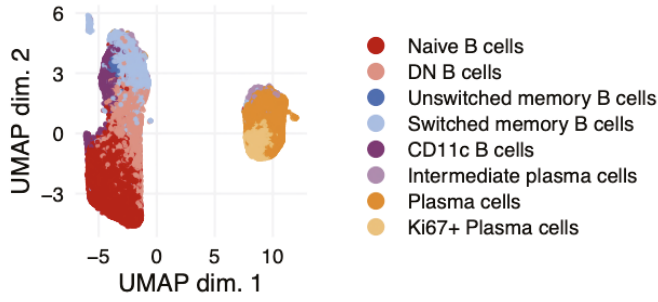
B

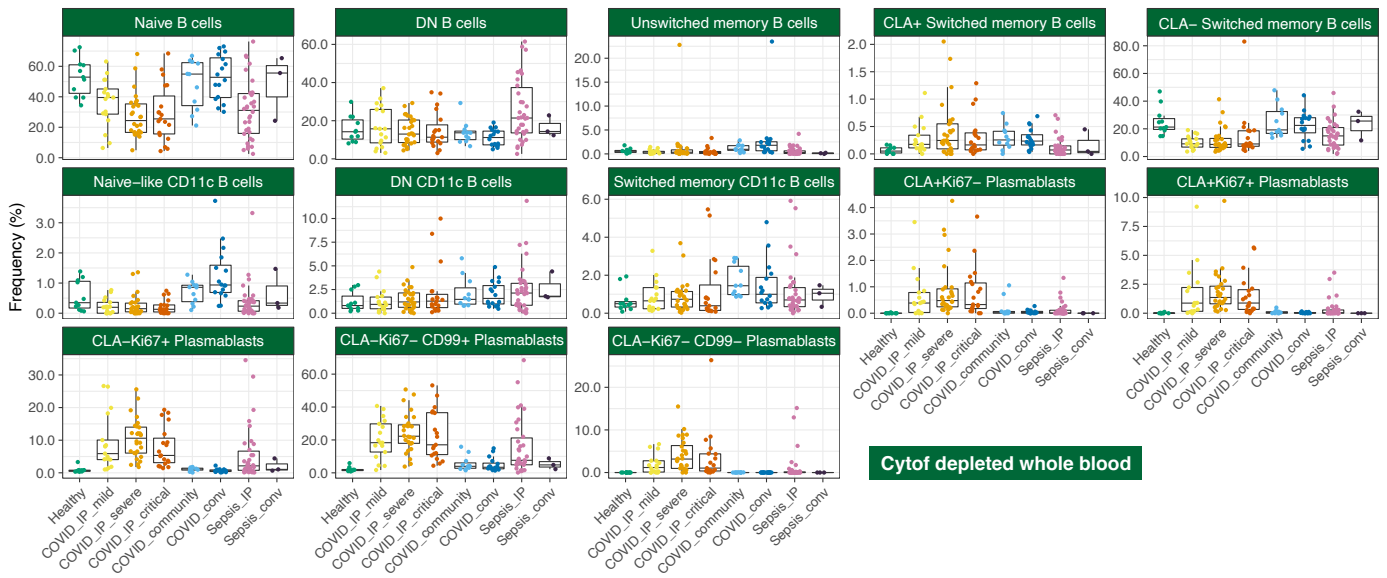


C

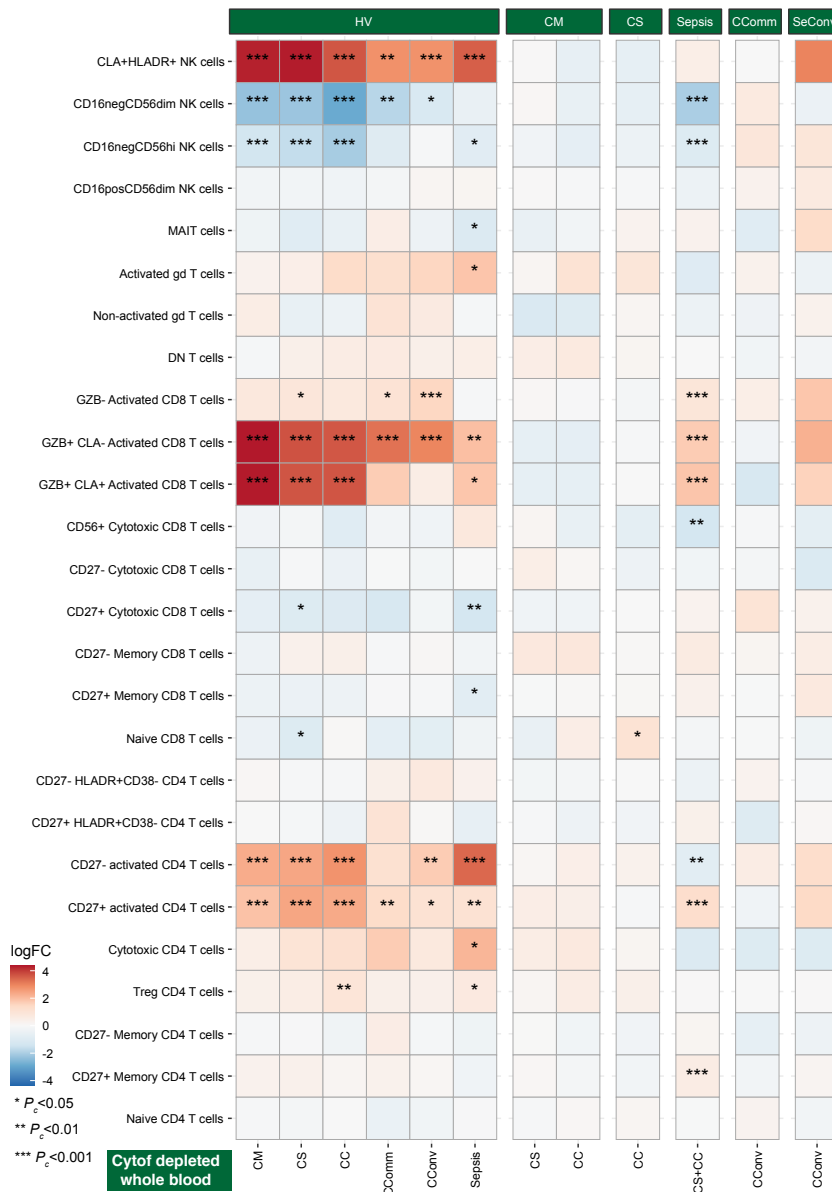
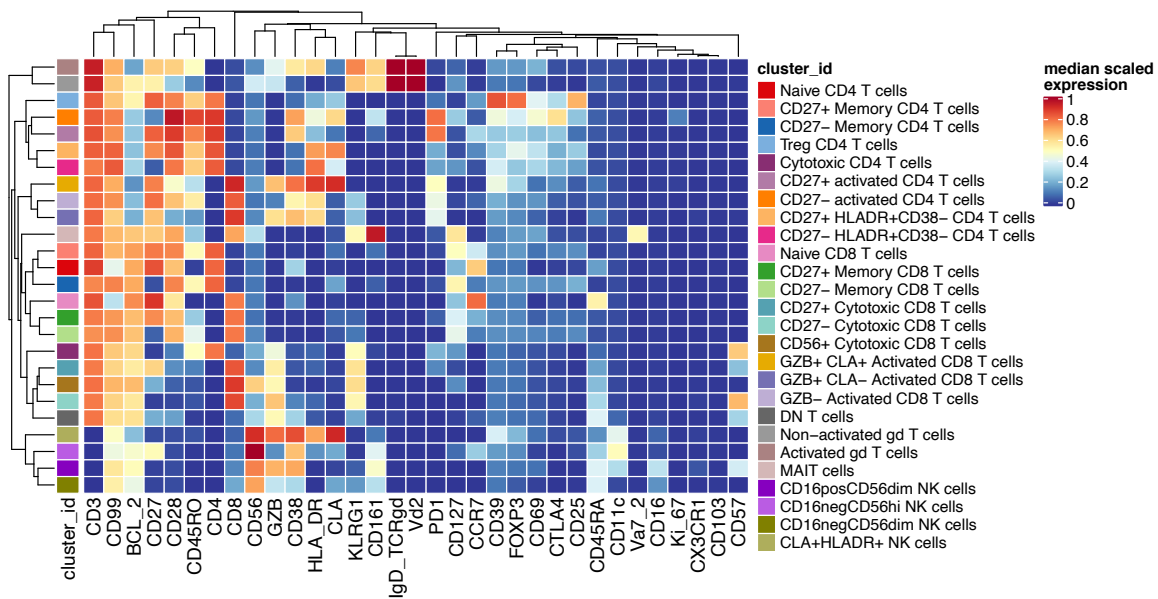


7: Myeloid cell populations from whole blood (depleted) assayed by single cell mass cytometry. (A) Overall populations. (B) Fine scale populations. (C) differential abundance analysis. Related to STAR Methods: Mass cytometry data analysis: differential abundance analysis.



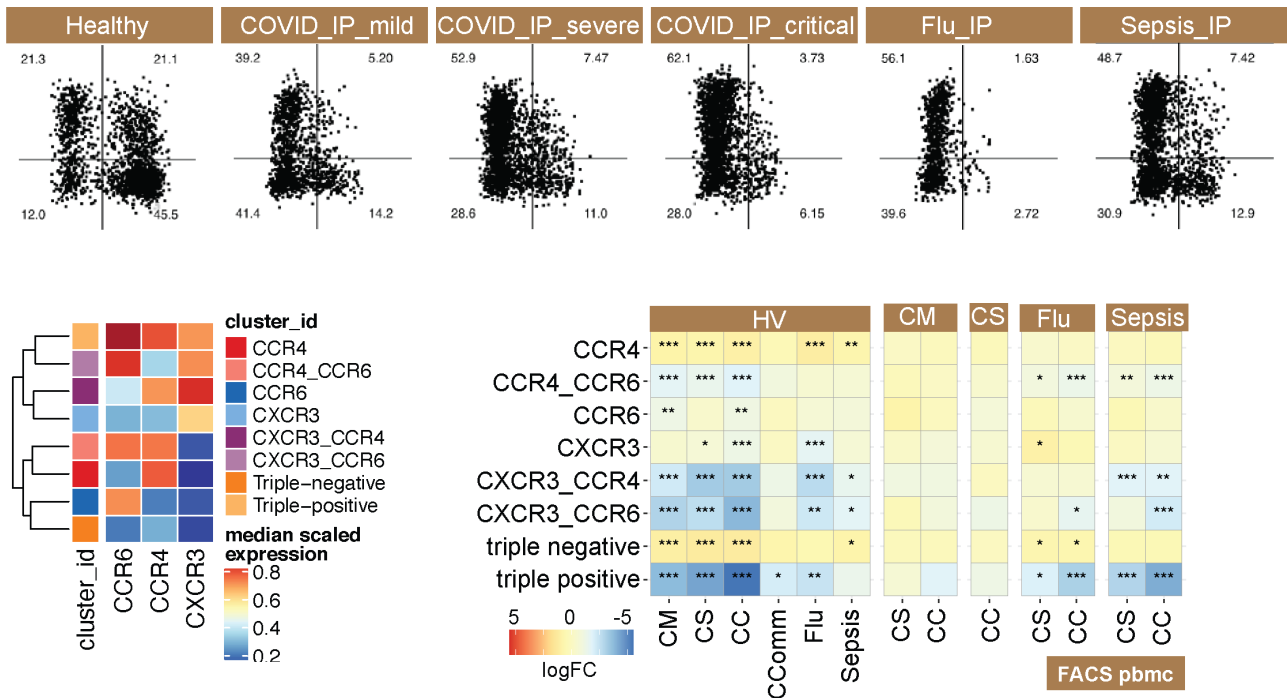


8: Single cell mass cytometry (CyTOF) compositional analysis showing UMAP, clustering and differential abundance of major B cell populations. Related to STAR Methods: Mass cytometry data analysis: differential abundance analysis.



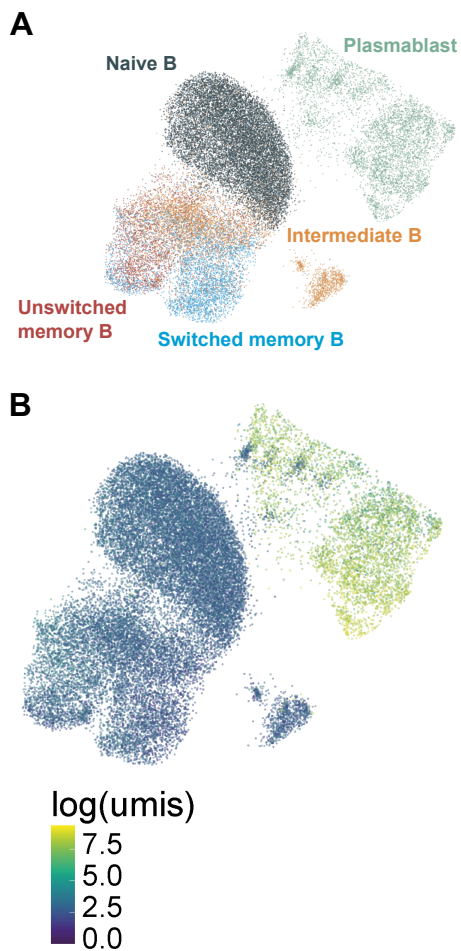
9: Phenotype of the T/NK cell populations assayed by single cell mass cytometry. (A) cell clustering (B) differential abundance analysis. Related to STAR Methods: Mass cytometry data analysis: differential abundance analysis.

Multicolor flow cytometry analysis

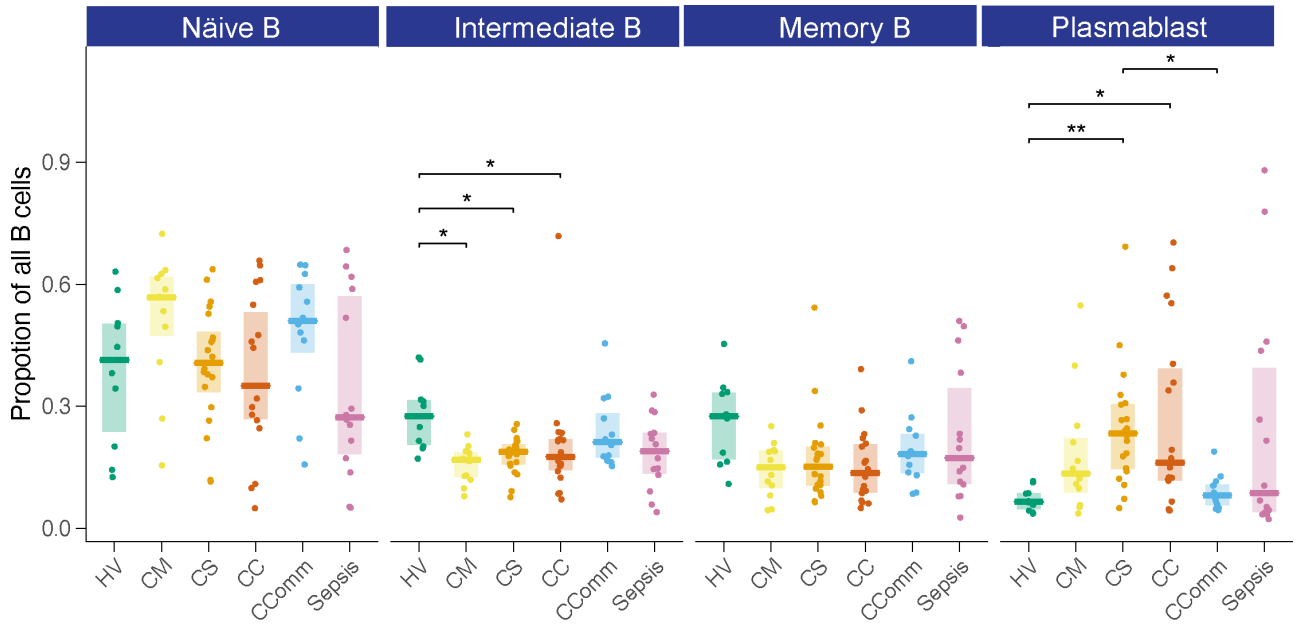


10: Phenotype and frequency of subsets of memory CD4 T cell subsets defined based on the expression of CCR4, CCR6 and CXCR3. PBMCs assayed using multicolor flow cytometry analysis. Dotplots, clustering and heatmap. Relates to Figure S4A-C. Related to STAR Method: Flow cytometry data analysis.

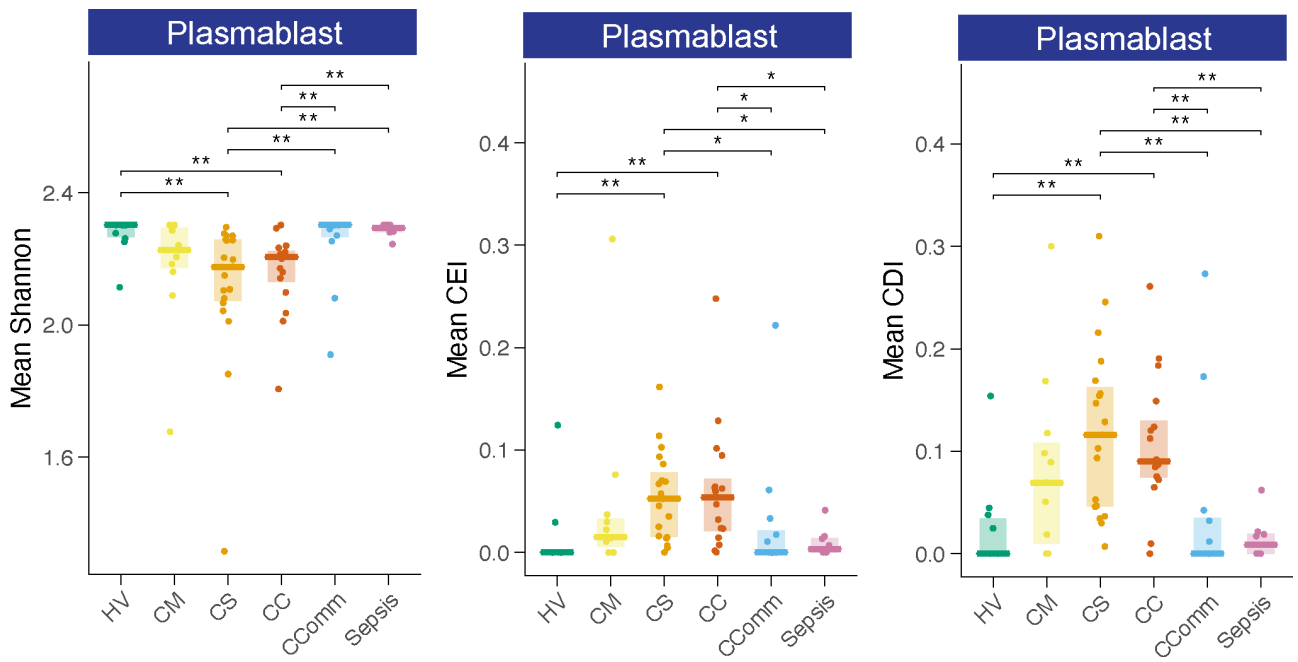
Repertoire analysis



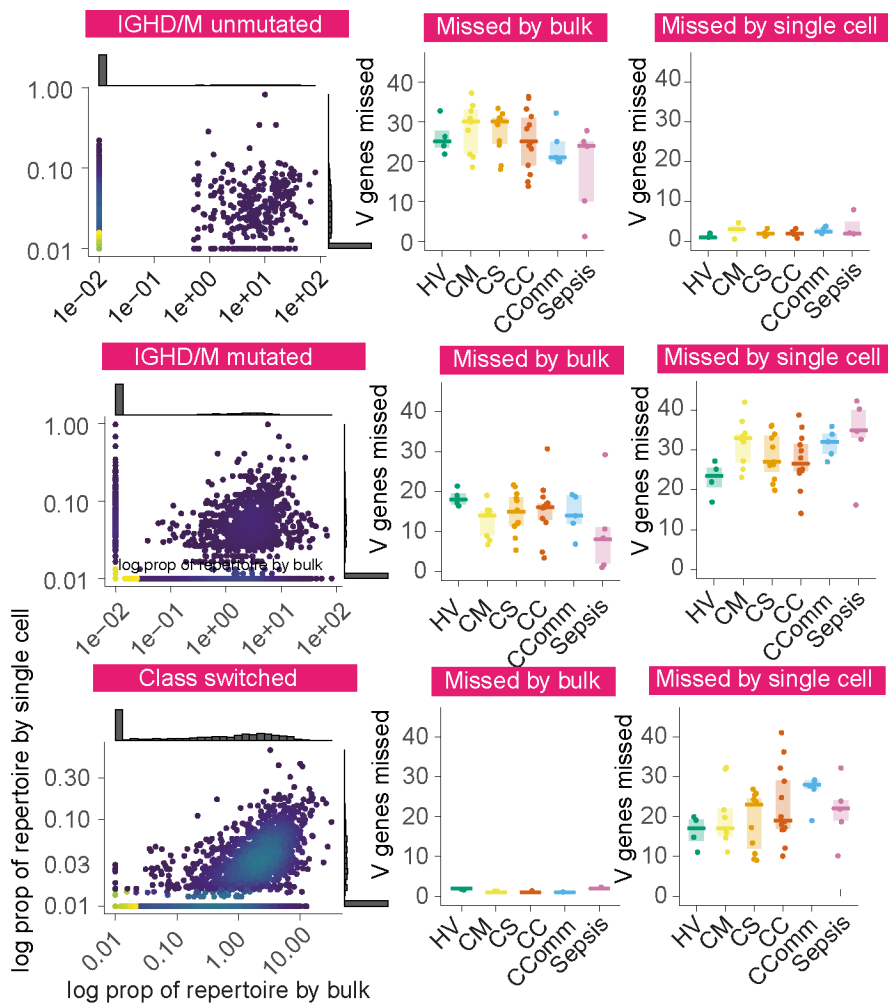
11: UMAP embedding B cell repertoire analysis (A) UMAP embedding with cluster identities from CITE-seq (B) UMAP embedding of all B cells from single cell VDJ dataset. As expected, PB showed the highest BCR expression in the CITEseq dataset. Color scale in panel B depicts log total UMIs per VDJ sequence. Related to STAR Methods: Repertoire analysis: additional pre-processing of scBCR-seq data.



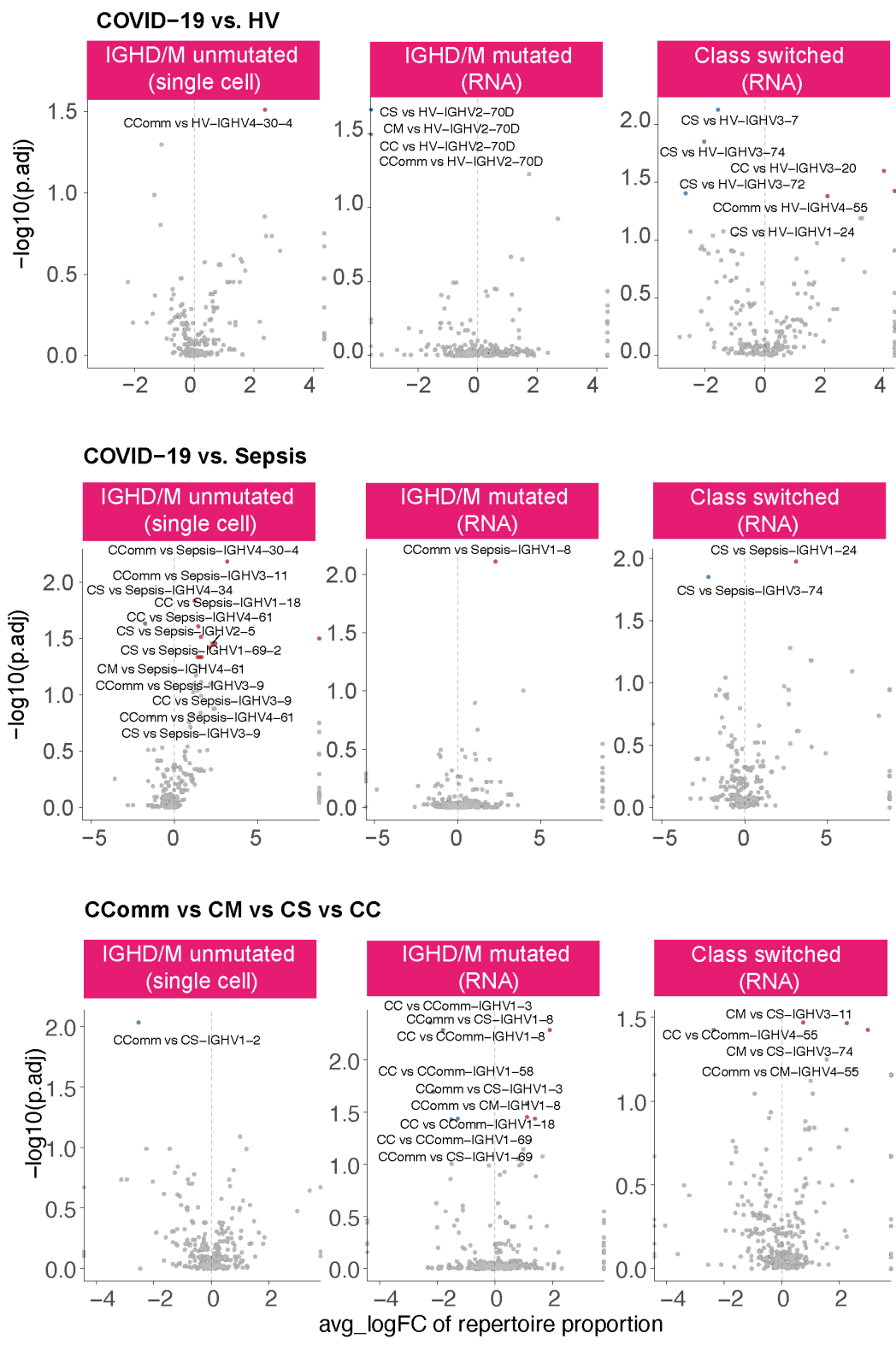
13: Cluster proportions. Related to STAR Methods: Repertoire analysis: RNA-velocity B cell analysis.



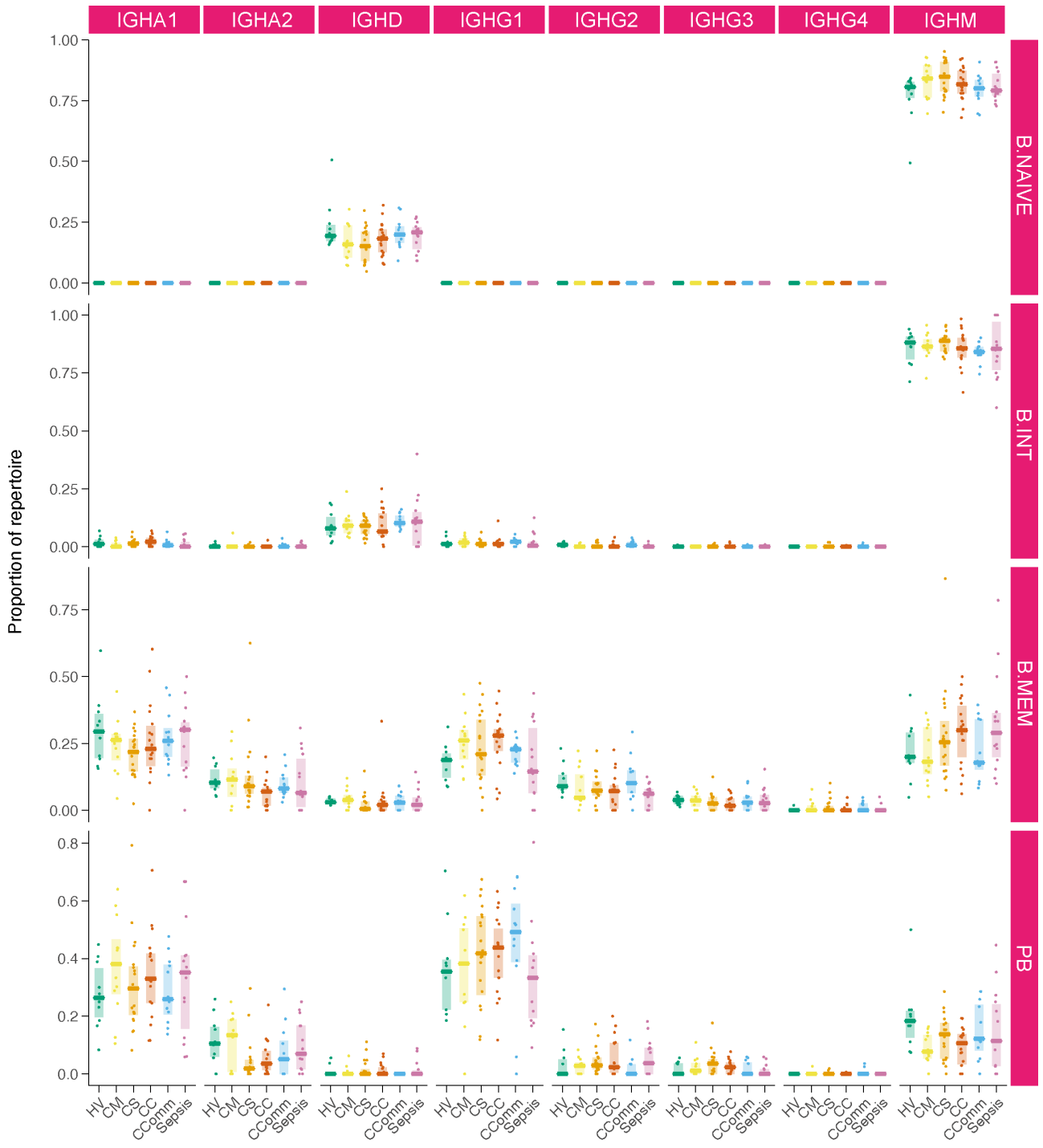
14: Mean plasmablast diversity indices by comparator group; clonal expansion index, CEI, clonal diversification index, CDI. Related to STAR Methods: Repertoire analysis: RNA-velocity B cell analysis.



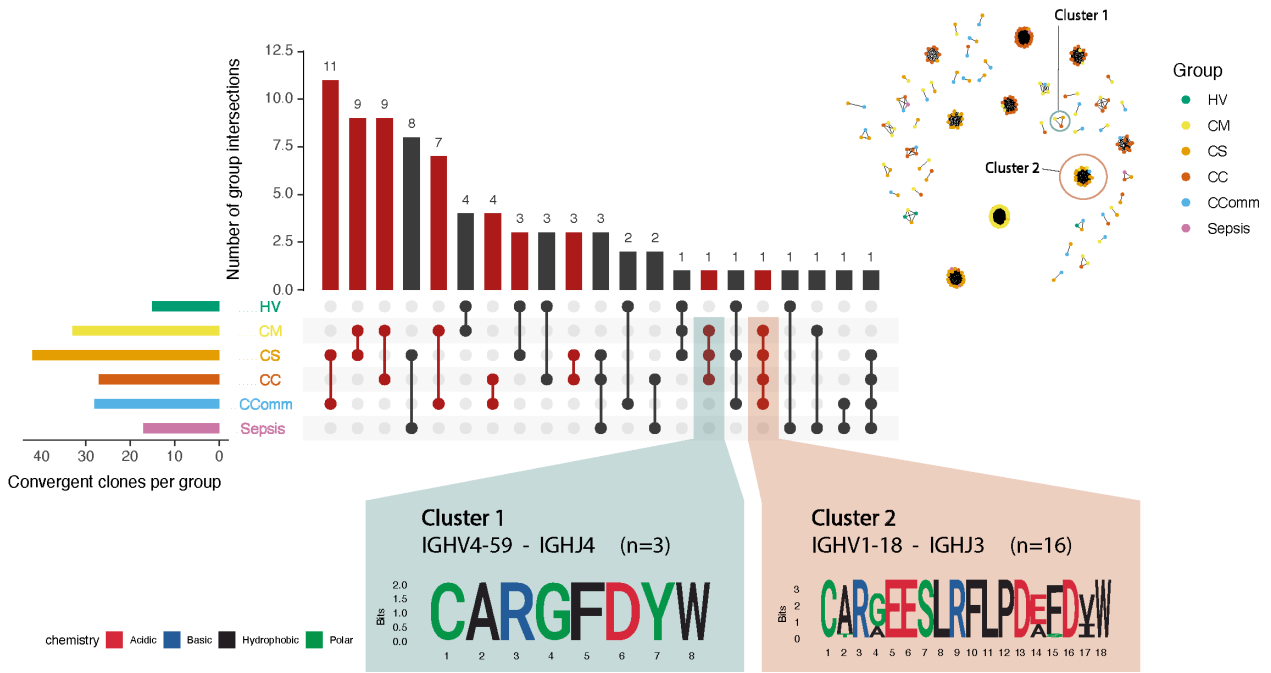
15: Correlation analysis of IGHV genes detected by single cell VDJ data and RNA VDJ data, within the (top) IGHD/M unmutated, (middle) IGHD/M mutated and (bottom) class-switched VDJ sequences. Scatter plots, with marginal histograms, depict log proportions of repertoires detected and missed by both datasets. Boxplots to the right depict number of IGHV genes missed by RNA (bulk) and single cell VDJ data. Related to STAR Methods: Repertoire analysis: RNA-velocity B cell analysis.



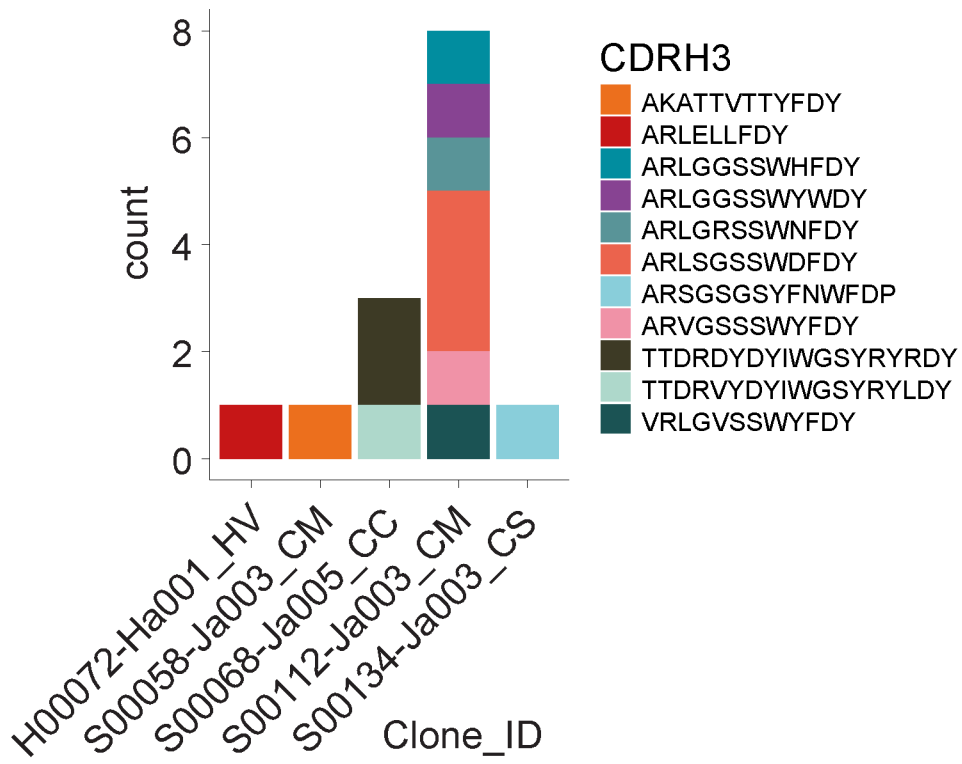
16: Volcano plots of log₂ fold change of IGHV gene usage of IGHD/M unmutated sequences (derived from single cell VDJ data), IGHD/M mutated sequences (derived from RNA VDJ data), class-switched sequences (derived from RNA VDJ data). Top panel depicts significant genes across pairwise comparisons of COVID-19 groups vs. healthy volunteers. Middle panel depicts significant genes across COVID-19 vs sepsis groups. Bottom panel depicts significant genes across COVID-19 severity groups. All significant pairwise comparisons are derived from Dunn tests post Kruskal Wallis testing. Related to STAR Methods: Repertoire analysis: RNA-velocity B cell analysis.



17: Proportion of constant region genes across B cell clusters per study group. Related to STAR Methods: Repertoire analysis: RNA-velocity B cell analysis.



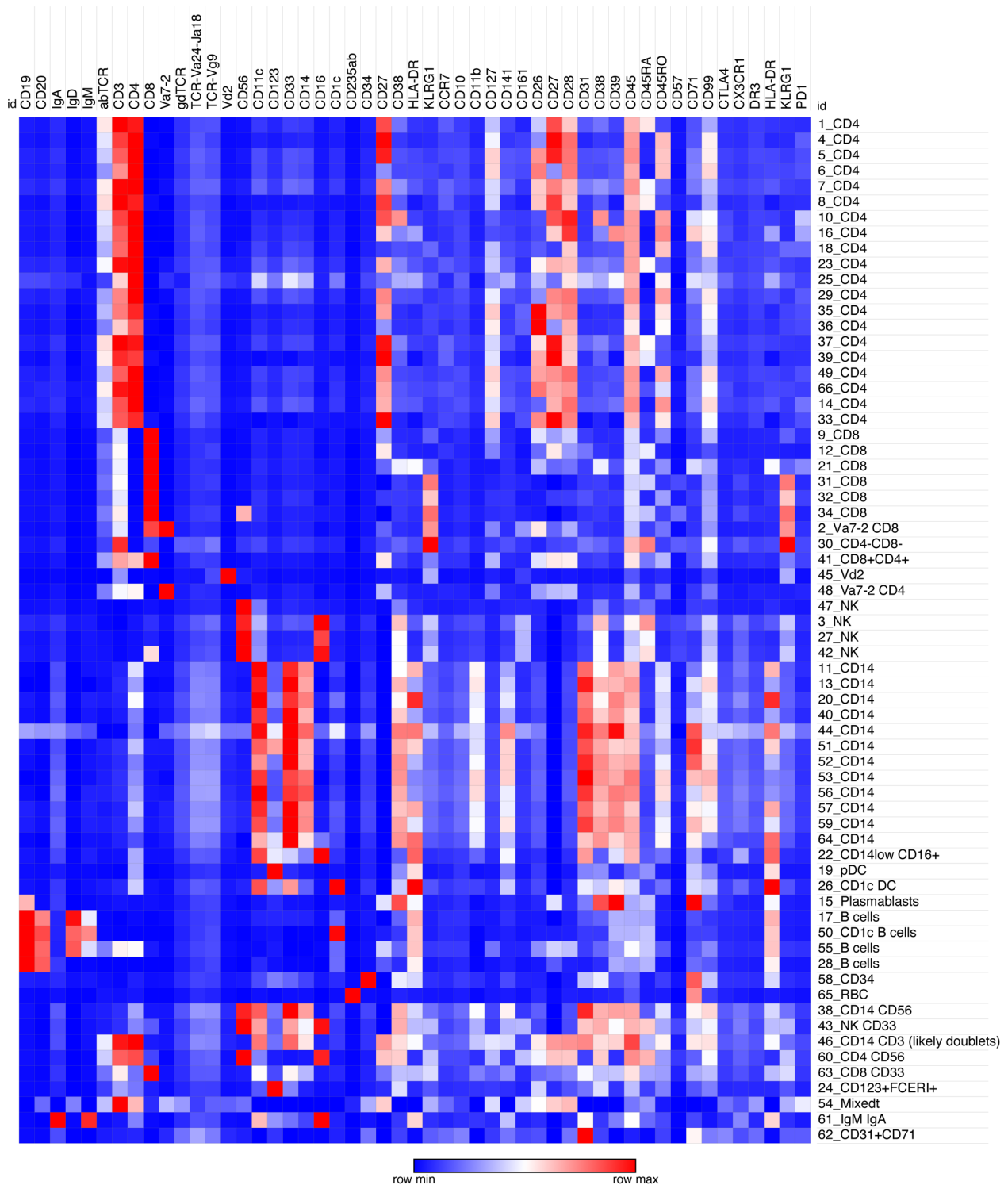
18: Clonal overlap across comparator groups with total number of convergent clones per group shown with clonal network depicting distribution of convergent clusters (inset) and sequence logos of COVID-19 exclusive clusters (with IGHV/J usage and number of members). Related to STAR Methods: Repertoire analysis: RNA-velocity B cell analysis.



19: Cumulative bar chart of the frequencies of known SARS-CoV-2 binding BCRs per patient group. Each section represents an individual patient. Related to STAR Methods: Repertoire analysis: RNA-velocity B cell analysis.

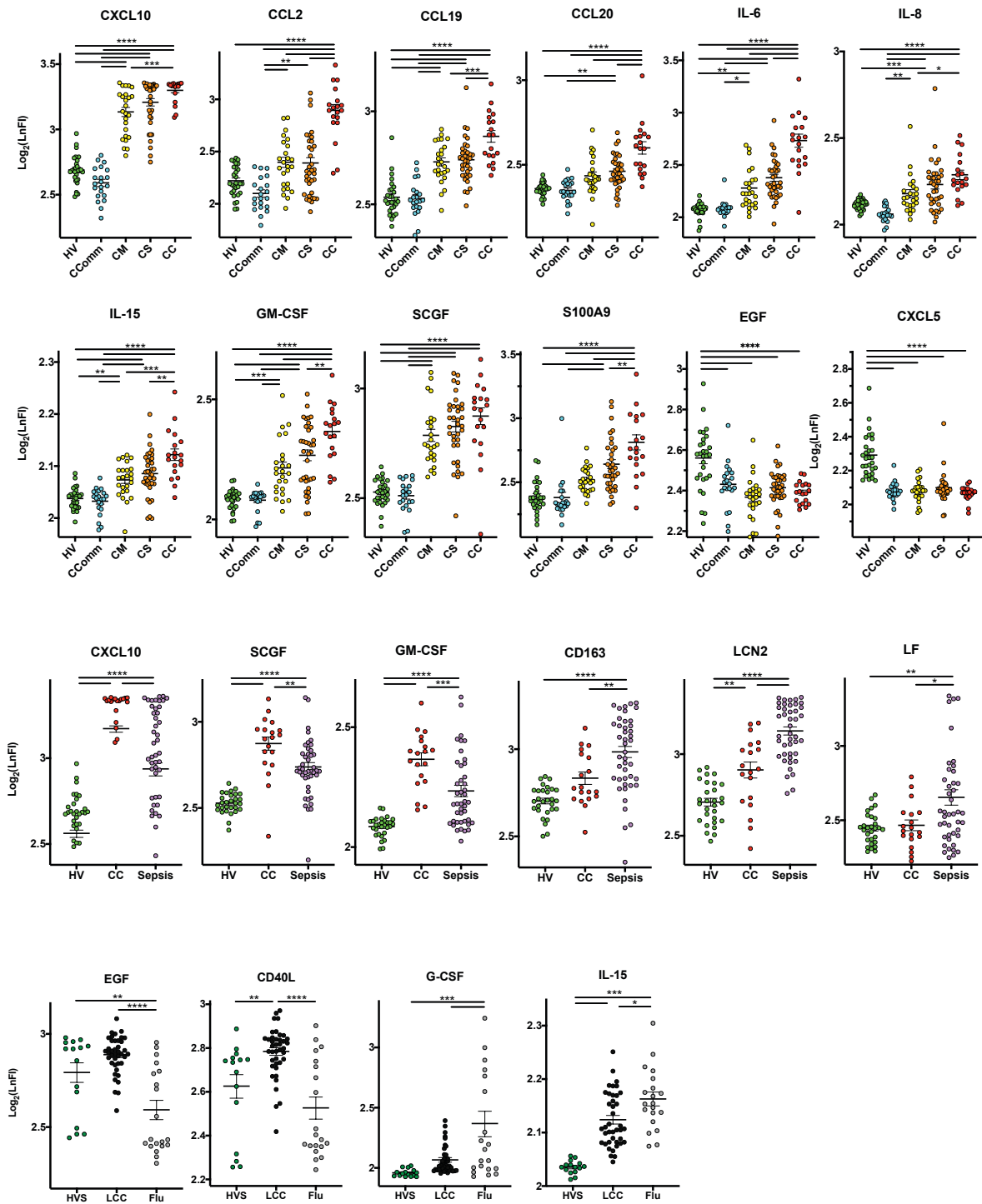
Proteomics

Clustering of surface protein (ADT) data

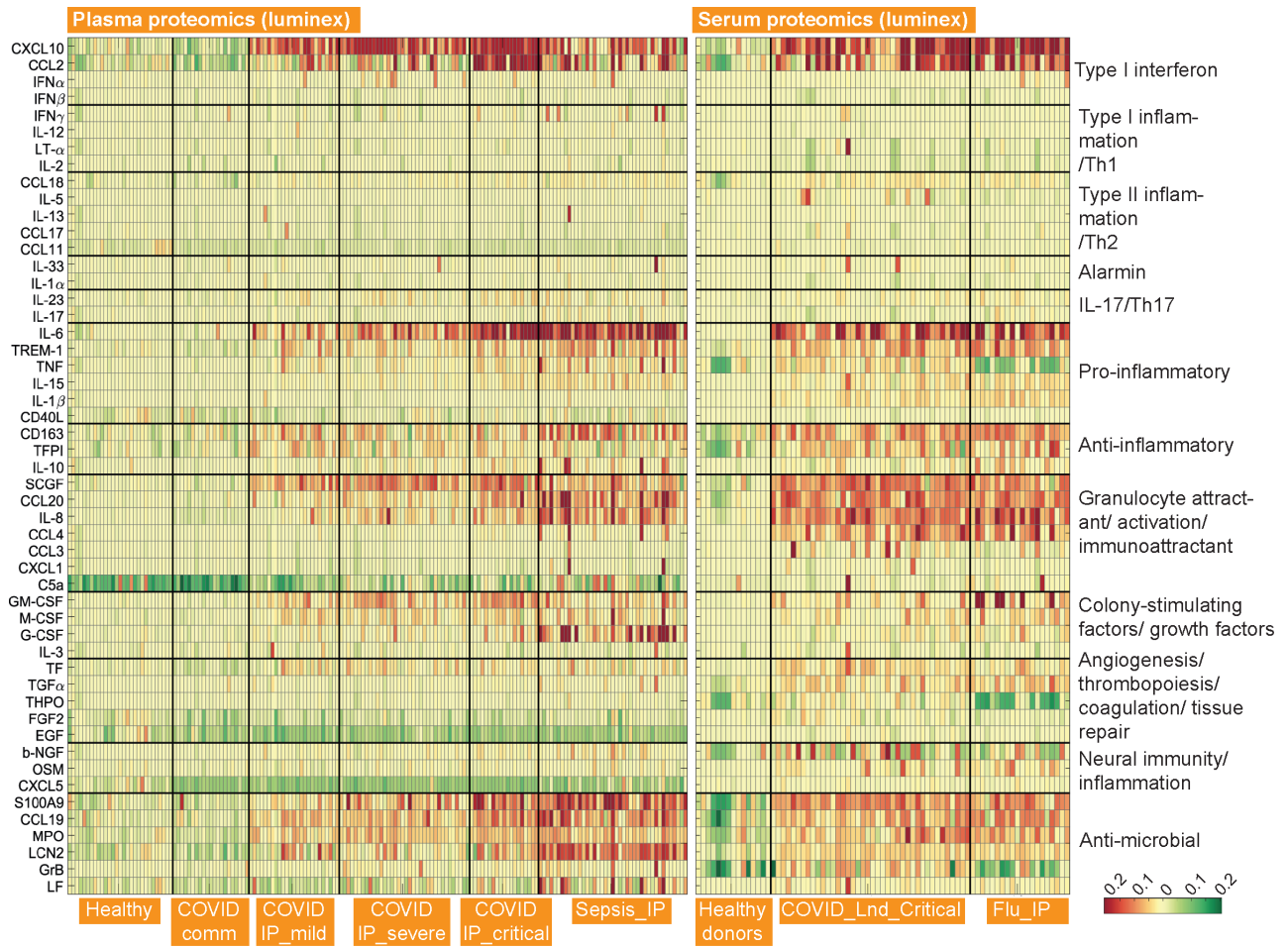


20: Clustering of surface protein (ADT) data. Initial cytoplasmic clustering of the CITE-seq dataset by ADT surface phenotype based on n=192 ADT tags. Columns: a selection of informative surface proteins (top labels), rows: Cytoplasmic cluster numbers and assigned phenotypes (right labels). Related to Figures 1B,C; STAR Methods: CITE-seq: Pre-processing and analysis of the surface protein (ADT) data; and Data S5: Multimodal annotation of CITE-seq data.

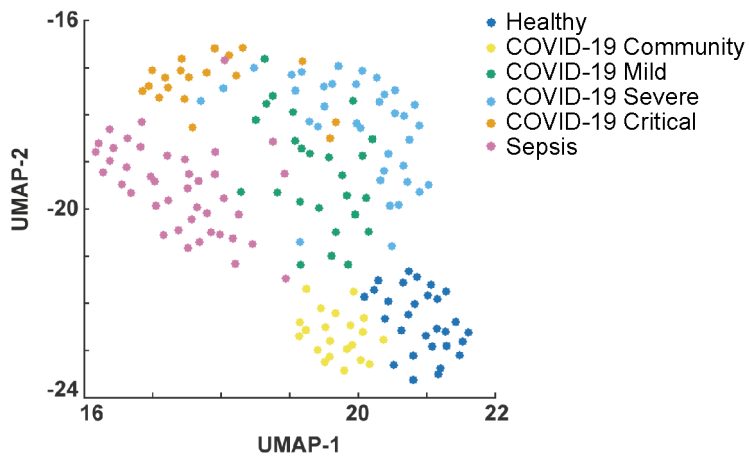
Plasma and serum proteins assayed by Luminex



21: Plasma protein abundance for specific proteins assayed by Luminex assay. Individual protein abundance across the comparator groups shown. Related to STAR Methods: Luminex data analysis: Cytokine enrichment profile analysis.

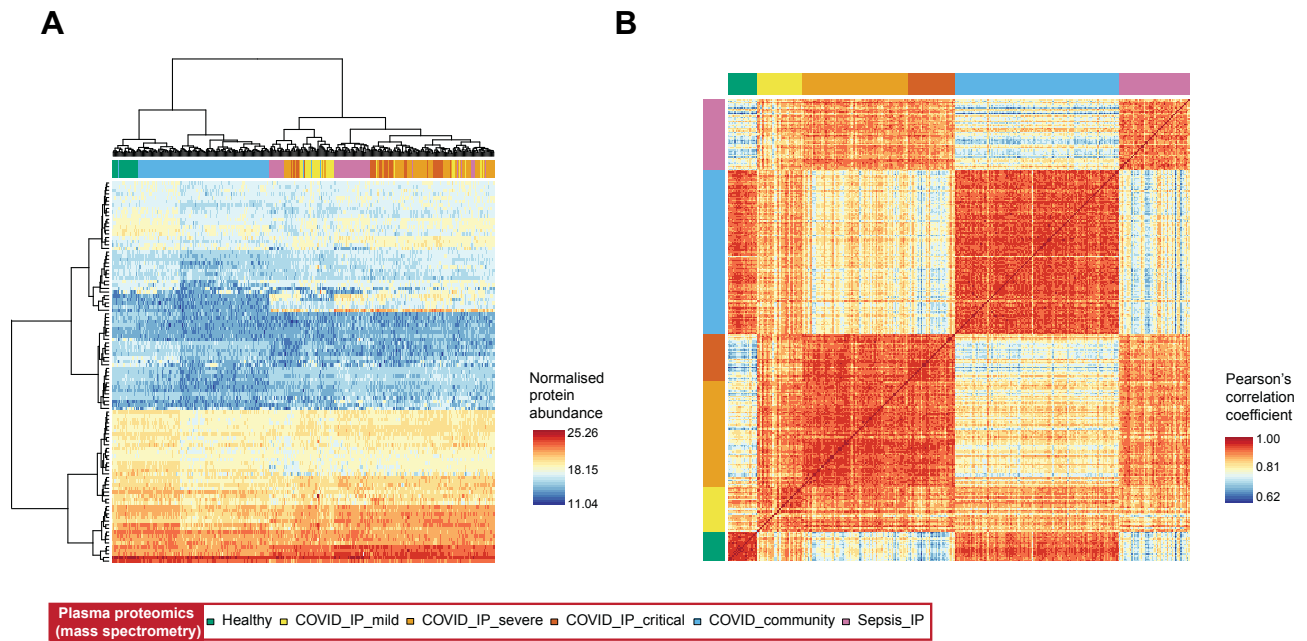


22: Heat map showing abundance of plasma and serum proteins by disease groups assayed using Luminex. Related to STAR Methods: Luminex data analysis: heatmap.

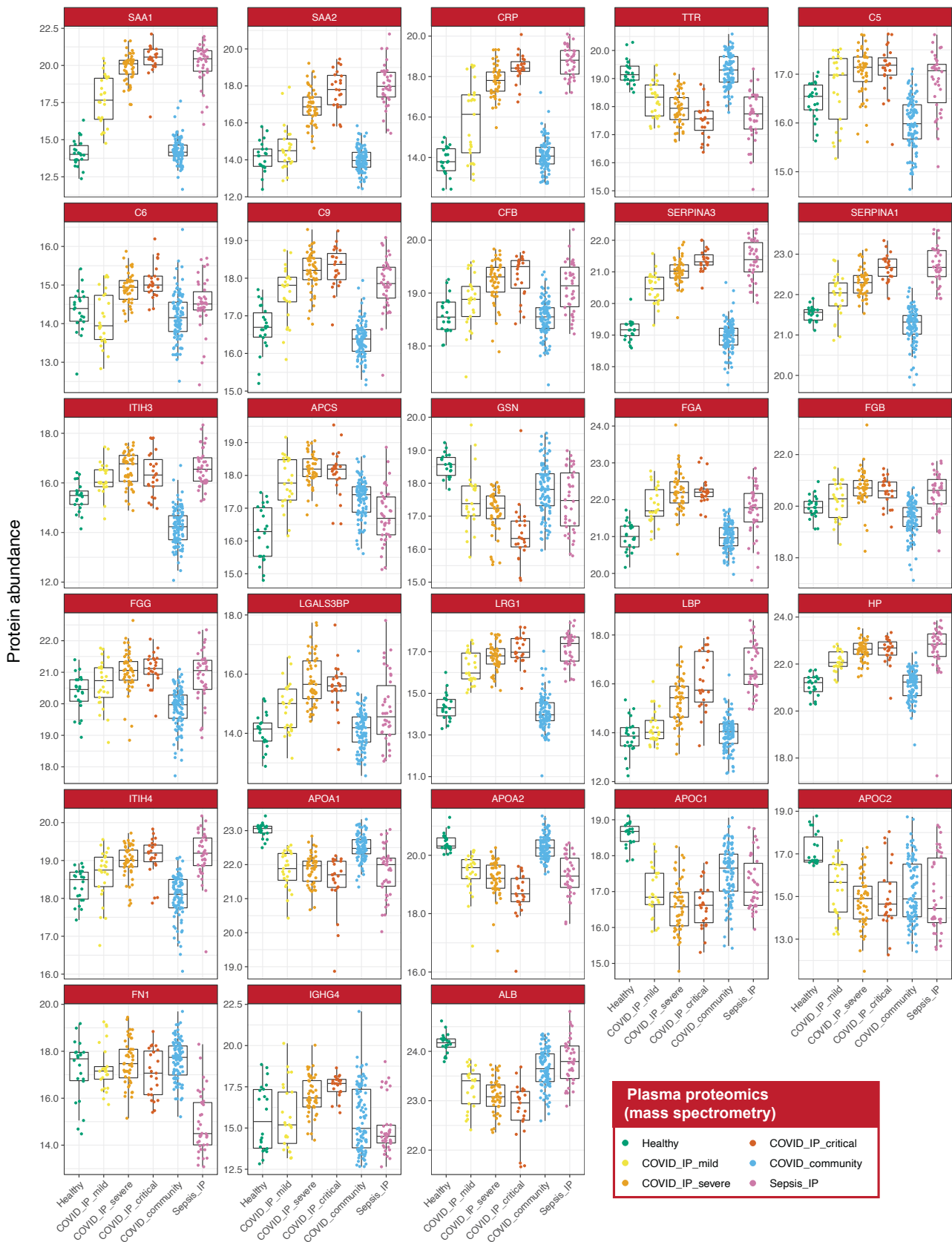


23: UMAP of plasma proteins assayed by Luminex assay, colored by comparator group.
Related to STAR Methods: Luminex data analysis: uniform manifold projection.

Plasma proteins assayed by HT-LC-MS/MS mass spectrometry



24: Unsupervised hierarchical clustering and supervised correlation analysis of plasma proteins assayed by HT-LC-MS/MS mass spectrometry. (A) Unsupervised clustering analysis all samples (B) supervised correlation analysis all samples. Related to STAR Methods: Tims-TOF mass spectrometry analysis: statistical analysis.



25: Plasma protein abundance for specific proteins assayed by HT-LC-MS/MS mass spectrometry. Individual protein abundance across the comparator groups shown. Only one sample per patient at the maximal severity are plotted. Related to STAR Methods: [Tims-TOF mass spectrometry analysis.](#)